Cardiovasc Toxicol (2013) 13:194–207
DOI 10.1007/s12012-013-9198-y

Cardiovascular Toxicity of Different Sizes Amorphous Silica Nanoparticles in Rats After Intratracheal Instillation

Zhongjun Du · Dali Zhao · Li Jing · Guanqun Cui · Minghua Jin · Yang Li · Xiaomei Liu · Ying Liu · Haiying Du · Caixia Guo · Xianqing Zhou · Zhiwei Sun

Published online: 16 January 2013

Abstract The purpose of this work was to investigate the cardiovascular toxicity of different sizes and different dosages of silica nanoparticles in Wistar rats. The three silica nanoparticles (30, 60, and 90 nm) and one fine silica particles (600 nm) at three doses of 2, 5, and 10 (mg/Kg bw) were used in the present experiment. After intratracheal instillation for a total of 16 times, concentration of Si in hearts and serum was measured by inductively coupled plasma optical emission spectrometer. The hematology parameters were analyzed by an automated hematology analyzer, and the inflammatory reaction, oxidative stress, endothelial dysfunction, and the myocardial enzymes in serum were measured by kits. Our results showed intratracheal-instilled silica nanoparticles could pass through the alveolar-capillary barrier into systemic circulation. Concentration of Si in the heart and serum depended on the particles size and dosage. The levels of reactive oxygen species (ROS) at 5, 10 mg/Kg bw of the three silica nanoparticles were higher than the fine silica particles. Blood levels of inflammation-related high-sensitivity C-reactive protein and cytokines such as interleukin-1beta (IL-1β), interleukin-6 (IL-6), and tumor necrosis factor-alpha were increased after exposure to three silica nanoparticles at 10 mg/Kg bw. Moreover, the levels of IL-1β and IL-6 at 10 mg/Kg bw of silica nanoparticles (30 nm) were higher than the fine silica particles. Significant decrease in superoxide dismutase, glutathione peroxidase and significant increase in malondialdehyde were observed at 10 mg/Kg bw of the three silica nanoparticles. A significant decrease in nitric oxide (NO) production was induced which coincided with the reduction of nitric oxide synthase (NOS) activity and the excessive generation of ROS in rats. The levels of intercellular adhesion molecule-l and vascular cell adhesion molecule-l elevated significantly after exposure to three silica nanoparticles at 10 mg/Kg bw, which are considered as early steps of endothelial dysfunction. We conclude that cardiovascular toxicity of silica nanoparticles could be related to the particles size and dosage. Oxidative stress could be involved in inflammatory reaction and endothelial dysfunction, all of which could aggravate cardiovascular toxicology. In addition, endothelial NO/NOS system disorder caused by nanoparticles could be one of the mechanisms for endothelial dysfunction.

Keywords Silica nanoparticles · Cardiovascular toxicity · Inflammatory reaction · Oxidative stress · Endothelial dysfunction

Z. Du · D. Zhao · M. Jin · Y. Li · X. Liu · Y. Liu · H. Du · Z. Sun
Department of Toxicology, School of Public Health, Jilin University, Changchun 130021, Jilin, People's Republic of China
e-mail: duzj1981@163.com

L. Jing · C. Guo · X. Zhou (✉) · Z. Sun (✉)
School of Public Health and Family Medicine, Capital Medical University, Beijing 100069, People's Republic of China
e-mail: xianqingzhou@yahoo.com.cn

Z. Sun
e-mail: zwsun@hotmail.com; zwsun@ccmu.edu.cn

G. Cui
Respiratory Department, The China-Japan Union Hospital, Jilin University, Changchun 130033, Jilin, People's Republic of China

Introduction

Silica nanoparticles have been found to have extensive applications. However, the versatile biomedical use of silica nanoparticles could cause new side effects [1–3].

Ultrafine particles (UFPs, with aerodynamic diameter less than 100 nm) can translocate from the lung to the systemic circulation by crossing the alveolar-capillary barrier [4, 5]. Inhaled ambient ultrafine particles can be found in heart, bone marrow, liver, kidney, and even central nervous system [6]. This could cause direct cardiovascular effects including inflammation, endothelial injury, and activation of coagulation pathways and thrombus development.

Various studies have shown that, on an equal-mass basis, nanoparticles induce stronger toxic responses than larger-sized counterparts of the same chemical composition [2, 7]. Both cell culture and animal model studies indicated that the retention and clearance processes were quite different between inhaled ultrafine and coarse particles. Furthermore, ultrafine particles in particulate matter were documented to be the crucial cause of cardiorespiratory disorders [8, 9]. Epidemiologic studies revealed that increased levels of ambient nanoparticles were associated with an increase in morbidity, mortality, and incidence of cardiovascular diseases in humans [8]. Inhalation of ambient particulate matter can adversely affect normal lung function and trigger various cardiovascular effects [10]. Although the toxicity of silica nanoparticles on extra-pulmonary tissues, especially cardiovascular has gradually drawn attention, it has rarely been reported.

Endothelial dysfunction is believed to induce pathological changes in the cardiovascular system. It can be considered as a predictor and an initiating event of atherosclerosis and its complications [5, 11]. Endothelial homeostasis is hypothesized to be directly affected by nanoparticle. A number of nanoparticles have been shown to directly affect the endothelial system, including increase in the expression of intercellular adhesion molecule-1 (ICAM-1), vascular cell adhesion molecule-1 (VCAM-1), and E-selectin [12]. Silica nanoparticles were capable of producing reactive oxygen species (ROS), leading to cytokine release and apoptosis [13]. Moreover, ROS-mediated oxidative stress played an important role in the toxicity of nanoparticles [14]. Therefore, the production of ROS-related different sizes of nanoparticles has an important role in the cause of endothelial dysfunction [15]. Evidence from human and toxicological exposure studies suggest that oxidative stress and inflammation are most likely involved in particle-mediated cardiovascular effects [16]. Silica nanoparticles could induce oxidative stress, pro-inflammatory stimulation, and fibrogenesis in Wistar rats [17, 18].

Unfortunately, up to now, little is known about the biological effects of the cardiovascular system caused by silica nanoparticles, and biological effect mechanism remains unclear. In the present study, we investigated the cardiovascular toxicity of different sizes and different dosages of silica particles and its possible mechanism in rats, which will provide a scientific basis to evaluate the risk of silica particles in the ecosystem and to human health.

Materials and Methods

Reagents

All chemicals used were of analytical grade or of ultra-purity. Nitric acid (HNO_3) and hydrochloric acid (HCl) were purchased from J.T. Baker, the Netherlands. Calibration standard solution of silicon (Si) was purchased from Central Iron & Steel Research Institute, China. Deionized water (H_2O) was purified by a Millipore system (Milli-Q, 18.2 MUcm).

Silica Particles

Characterization of Amorphous Silica Particles

Silica particles of 30, 60, 90, and 600 nm in aqueous suspension were obtained from School of Chemistry, Jilin University, China. The particle sizes and distribution of silica particles were measured by transmission electron microscope (TEM) (JEOL, Japan). Dynamic light scattering (DLS) technique was employed using zeta electric potential granulometer (Nano ZS90, Malvern, UK) to examine the hydrodynamic sizes of silica particles in dispersion media. Crystal structure was characterized by Scintag XDS 2000 diffractometer (Scintag, Inc. Cupertino, CA, USA).

The major trace metal impurities in 30, 60, 90, and 600 nm silica particles were measured using a PerkinElmer ELAM DRC-e Inductively Coupled Plasma-Mass Spectrometry (ICP-MS) system (PerkinElmer, Wellesley, MA, USA). The ICP-MS conditions were set up as follows: vacuum pressure: 6.5×10^{-6} Torr; nebulizer gas flow: 0.98 l/min; ICP RF power: 1,200 W; lens voltage: 7.6 V; analog stage voltage: −1,700 V; pulse stage voltage: 1,100 V. The data are presented in Table 2. The results indicated that the purity of four sizes of silica particles was better than 99.80 %. The characterization results are shown in Fig. 1; Tables 1 and 2.

Endotoxin Determination of Silica Particles with LAL Test

To determine whether the particles and media were contaminated by endotoxin, the Limulus amebocyte lysate (LAL) test was performed [19]. After repeated examination of the tachypleus amebocyte lysate (TAL) (sensitivity: $\lambda = 0.125$ EU/ml, Zhanjiang A&C Biological Ltd, Zhanjiang, China) sensitivity and sample interference test,

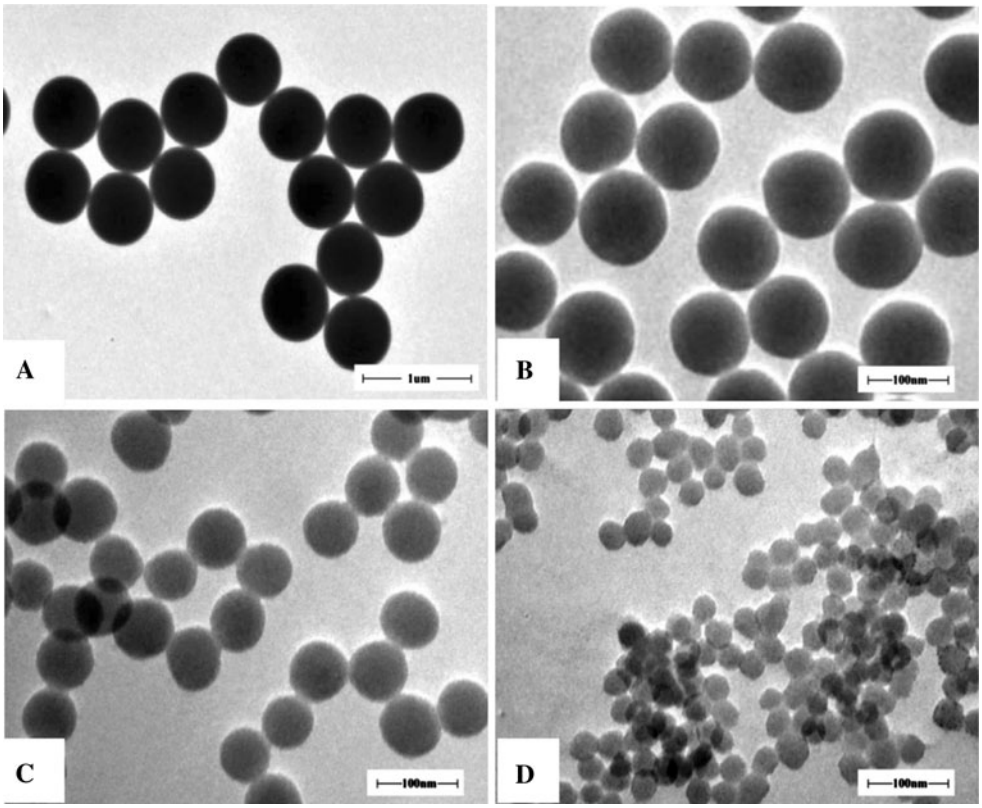

Fig. 1 Transmission electron microscopy images of silica particles. **a** Si600, **b** Nano-Si90, **c** Nano-Si60, and **d** Nano-Si30

Table 1 Characterization of silica particles

Characterization	Si600	Nano-Si90	Nano-Si60	Nano-Si30
Size and distribution nm (mean ± SD)	584.76 ± 24.83	92.30 ± 7.42	60.80 ± 4.36	27.26 ± 4.92
Hydrodynamic size in normal saline (nm)	678.0	136.4	99.5	71.4
Shape	Spheroidicity	Spheroidicity	Spheroidicity	Spheroidicity
Aggregation[a]	−	−	−	+
Crystalline structure	Amorphous	Amorphous	Amorphous	Amorphous
Endotoxin determination[b]	−	−	−	−

[a] (−) No aggregation, (+) aggregation, [b] (−) Endotoxin free

four tubes with 0.1 ml TAL reagent were used. 0.1 ml silica particles physiological saline solution was added to two tubes; meanwhile, 0.1 ml bacterial endotoxin test water provided by National Institute for the Control of Pharmaceutical and Biological Products (Beijing, China) and 0.1 ml working control standard endotoxin (government standard number: 201202, working standard number: 201301) were added to the other two tubes as negative control and positive control. All tubes were incubated for 1 h in a water bath at 37 ± 1 °C. After the test tube was slowly inverted 180°, it is positive and recorded as (+) if the gel in tube is not deformed and does not slip from the wall, whereas is negative and recorded as (−). Test is invalid when positive control is (−) or negative control is (+).

Experimental Animals and Experimental Design

Experimental Animals

Male Wistar rats with body weight of 180 ∼ 210 g were purchased from the Department of Experimental Animals, Norman Bethune College of Medicine JiLin University, China (The number for certificate of animals is SYXK (Ji)

Table 2 Metal impurity levels in silica particles

Elements	Al	K	Ca	Mg	Fe	Cu	Na	Zn	Pb	Mn
Nano-Si30	<40	<40	<40	<40	<40	<40	<40	<40	<40	<40
Nano-Si60	<40	<40	<40	<40	<40	<40	<40	<40	<40	<40
Nano-Si90	<40	<40	<40	<40	<40	<40	<40	<40	<40	<40
Si600	<40	<40	<40	<40	<40	<40	~40	<40	<40	<40

Twenty elements tested in our ICP-MS system and all of their levels were below the detection limits (40 ppb), except that of Na in 600 nm group. Ten elements not tabulated included V, Co, Ni, As, Se, Ag, Cd, Ti, Cs, U

2007-0011), and maintained under standard housing conditions (Temperature: 18–24 °C; Relative Humidity: 45 %; Light and Dark Cycle: 12 h:12 h). Food and water were provided ad libitum. All animal experiments were treated according to the protocols evaluated and approved by the ethical committee of Norman Bethune Department of Medicine Jilin University.

Experimental Design

Silica particles of 30, 60, 90, and 600 nm in aqueous suspension were obtained from School of Chemistry, Jilin University, China. Four sizes of silica particles suspensions were diluted by adding normal saline, so as to obtain mass concentrations of 2 mg/Kg bw (low dose), 5 mg/Kg bw (middle dose), and 10 mg/Kg bw (high dose), respectively. Rats were randomly divided into 13 groups with 6 rats per group (normal control, 0.9 % physiological saline); four sizes of silica particles with low-dose group (2 mg/Kg bw), middle-dose group (5 mg/Kg bw), and high-dose group (10 mg/Kg bw), respectively.

Animals Exposure to Silica Particles

Rats were mildly anesthetized with ether, and rats faced away from the operator. Taking otoscope into the rat oral and exposing tracheal opening, the light shined in the otoscope, then V-shaped opening and closing white ring (vocal cords) with breathing could be seen. The operator fixed the otoscope, when the V-shaped was mouth open, the blunt puncture needle passed by assistant was inserted into the trachea about 1–1.5 cm, and then the needle had reached the middle of the trachea. Assistant connected the injection syringe to the puncture needle, withdrawing if any bubbles, and then we could inject the test solution into trachea. The intratracheal instillations were well tolerated and no adverse effects were observed during the study period. At the end of the experimental with exposure to 16 times every other day, and intratracheal instillations of 0.2 ml corresponding concentration of particles suspension for every time.

Animal Autopsy

Rats were weighed and anesthetized with 10 % chloral hydrate intraperitoneal. Some blood was collected through the aorta blood collection and centrifuged at 3,000r/min for 10 min at 4 °C, and the supernatant serum was collected for analysis. The other blood was collected in tubes containing the anticoagulant ethylenediamine tetraacetate (K_2EDTA). Part of the blood was used for blood cell count, and the remaining blood with anticoagulant was centrifuged with 3,000r/min for 10 min at 4 °C, and plasmas were collected. Then, the rats were killed. Hearts were weighed, and tissue samples were homogenized and frozen for the determination of silica content. Serum and plasma were stored at −20 °C until analysis.

Measurement of Si Concentration in the Samples with ICP-OES

Homogenized heart samples (0.5 g) or serum samples (0.2 ml) were weighed into Teflon pressure digestion vessels of the microwave system (MDS-6, Milestone, Italy). Into the Teflon pressure digestion vessels, 4 ml HNO_3 and 1 ml H_2O_2 were added. The mixture was treated under microwave conditions, including three stages: (1) 5 min: 20–90 °C; (2) 10 min: 90–170 °C; (3) 30 min: 170–200 °C. Afterward, the mixture was transferred to 15-ml PET plastic tube, deionized water with a little washing 3 ~ 4 times a digestion tank, and deionized water (H_2O) was added to a total volume of 10 ml. The total solution was shortly shaken by hand. Then, Si contents of the samples were analyzed by inductively coupled plasma atomic emission spectrometry (ICP-OES, PerkinElmer, USA).

Si standard solution will be gradually diluted by 5 % nitric acid medium to 0.25, 0.5, 1.0, 2.0, 4.0, and 8.0 μg/ml. Determination of blank and standard solution series under the optimized experimental conditions and apparatus draws standard curve automatically. The linear correlation coefficient is $r \geq 0.9999$. Detection wavelength of Si is 251.61 nm, and the limit of detection is 15 ppb. Data were represented in μg/ml blood serum and μg/g organ.

Biochemical Analyses

Levels of tumor necrosis factor-α (TNF-α), interleukin-6 (IL-6), interleukin-1β (IL-1β), reactive oxygen species (ROS), MB isoenzyme of creatine kinase (CK-MB), endothelin-1(ET-1), P-selectin (Groundwork Biotechnology diagnosticate, USA), D-dimer, Intercellular adhesion molecule-1 (ICAM-1), Vascular cell adhesion molecule-1(VCAM-1), (RD Biosciences, Inc, USA), inducible nitric oxide synthase (iNOS), endothelial nitric oxide synthase (eNOS), (Jiancheng, Nanjing, China), and high-sensitivity C-reactive protein (hs-CRP), (Life diagnostics Inc, PA, USA), were measured by ELISA according to the manufacturers' protocols. The absorbances at 450 nm were measured by using Synergy 2 multi-mode microplate reader (BioTek, USA). Levels of superoxide dismutase (SOD), glutathione (GSH), glutathione peroxidase (GSH-Px), malondialdehyde (MDA), lactate dehydrogenase (LDH), nitric oxide (NO), and nitric oxide synthase (NOS) were measured by commercial kit (Jiancheng, Nanjing, China) according to the manufacturers' protocols. The absorbances at 550 nm (SOD), 412 nm (GSH), 412 nm (GSH-Px), 532 nm (MDA), 440 nm (LDH), 550 nm (NO), and 530 nm (NOS) were measured by using UV-752 Spectrophotometer (LengGuang, China). The quantity of white blood cells (WBC), red blood cells (RBC), platelets (PLT), and the concentration of hemoglobin (HGB) in the blood samples collected on day were analyzed by an automated hematology analyzer (model KX-21NV, Sysmex Corporation, Kobe, Japan).

Statistical Analyses

Data were expressed as mean ± SD and significance was determined by using one-way analysis of variance (ANOVA) followed by least significant difference (LSD) test to compare the differences between groups. The value of $p < 0.05$ was considered significant.

Results

Characterization of Silica Particles

The hydrodynamic sizes of four amorphous silica particles were measured in 0.9 % physiological saline as stock media to reflect their dispersion throughout the experiments. Owing to the Van der Waals force and hydrophobic interaction with surrounding media, silica particles generally had the larger hydrodynamic size in dispersion media than their original size. In addition, Si600 (A), Nano-Si90 (B), and Nano-Si60 (C) exhibited very good monodispersity in the experiment, while Nano-Si30 (D) agglomerated slightly due to their high surface activity.

The Concentration of Si Measured in the Hearts and Serum

As shown in Table 3, in the hearts and serum, compared with the control group, the concentration of Si was increased significantly except the low dose of Si600. At the same-size particle groups, compared with the low-dose groups, a significant increase in the concentration of Si measured in the hearts and serum was found in high-dose groups of Si 600, Nano-Si90, Nano-Si60, and Nano-Si30. And the Si concentration in the serum of middle-dose groups of Nano-Si90, Nano-Si60, and Nano-Si30 and in the hearts of the middle-dose groups of Nano-Si30 was higher than those in the low-dose groups. At the same-dose groups, the concentration of Si in serum in all experimental groups of Nano-Si90, Nano-Si60, and Nano-Si30 and in the hearts in high-dose groups of Nano-Si90 and Nano-Si60 was significantly up-regulated when compared with Si600 groups. Moreover, the higher concentration of Si in hearts was found in middle-dose and high-dose groups of Nano-Si30.

Changes of Hematology Parameters of Rats Induced After Intratracheal Instillation of Silica Particles

As shown in Fig. 2, compared with the control group, there was a significant increase in WBC and PLT levels. At the

Table 3 Si concentration of hearts and serum for rats after intratracheal instillation of silica particles ($\bar{x} \pm$ SD, $n = 6$)

Group	(A) serum (μg/ml)	(B) heart (μg/g)
Control	2.38 ± 0.81	0.60 ± 0.07
600 nm-2	6.33 ± 2.26[a]	0.78 ± 0.12
600 nm-5	7.74 ± 1.37[a]	1.02 ± 0.12[a]
600 nm-10	11.07 ± 0.99[ab]	1.10 ± 0.20[ab]
90 nm-2	10.65 ± 1.43[ad]	0.86 ± 0.10[a]
90 nm-5	15.25 ± 3.07[abd]	0.94 ± 0.14[a]
90 nm-10	25.84 ± 2.31[abcd]	1.28 ± 0.21[abcd]
60 nm-2	10.03 ± 1.15[ad]	0.82 ± 0.12[a]
60 nm-5	15.73 ± 1.61[abd]	0.98 ± 0.10[a]
60 nm-10	24.44 ± 2.72[abcd]	1.20 ± 0.37[abcd]
30 nm-2	14.88 ± 3.44[ad]	0.91 ± 0.18[a]
30 nm-5	18.15 ± 1.86[abd]	1.37 ± 0.19[abcdef]
30 nm-10	26.31 ± 3.82[abcd]	2.01 ± 0.13[abcdef]

The concentration of Si measured after exposure to 600, 90, 60 and 30 nm of silica particles with concentrations from 2 to 10 mg/Kg bw. [a] $p < 0.05$, versus control group; [b] $p < 0.05$, versus the same-size group (2 mg/Kg bw); [c] $p < 0.05$, versus the same-size group (5 mg/Kg bw); [d] $p < 0.05$, versus the same-dose group (600 nm); [e] $p < 0.05$, versus the same-dose group (90 nm) and [f] $p < 0.05$, versus the same-dose group (60 nm)

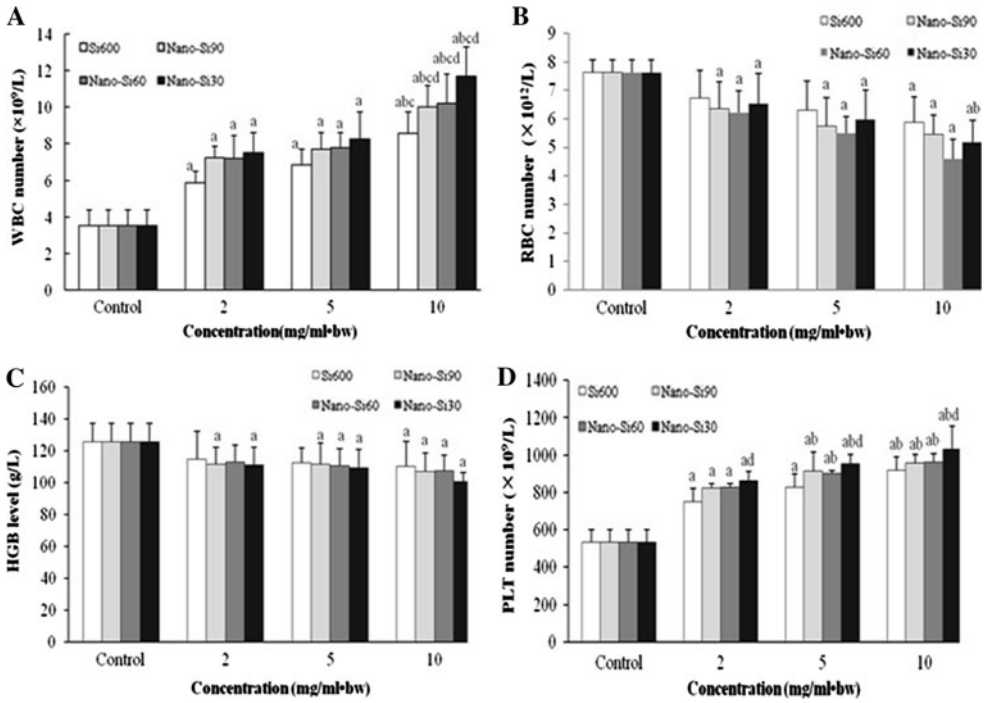

Fig. 2 The values of hematological after exposure to 600, 90, 60 and 30 nm of silica particles with concentrations from 2 to 10 mg/Kg bw. **a** WBC number; **b** RBC number; **c** HGB level; **d** PLT number. The results manifested that hematological values changed in both dose-dependent and size-dependent manner. [a] $p < 0.05$, versus control group; [b] $p < 0.05$, versus the same-size group (2 mg/Kg bw); [c] $p < 0.05$, versus the same-size group (5 mg/Kg bw); [d] $p < 0.05$, versus the same-dose group (600 nm)

same-size particle groups, the WBC numbers in the high-dose groups of the four sizes of particles were higher than those in the low- and the middle-dose groups. At the same-dose groups, the WBC numbers in high-dose groups of Nano-Si90, Nano-Si60, and Nano-Si30 were significantly higher than the Si600. And the WBC number in low- and middle-dose groups of Nano-Si30 and the low-dose groups of Nano-Si90 were also significantly higher than those of the Si600. The higher PLT number was found in high-dose groups of the four sizes of particles and middle-dose groups of Nano-Si90, Nano-Si60, and Nano-Si30 comparing with low-dose groups. There was a significant increase in PLT numbers of Nano-Si30 groups with concentrations from 2 to 10 mg/Kg bw comparing with the Si600 groups. A significant decrease in the RBC number and the concentration of HGB was found in Nano-Si90, Nano-Si60, Nano-Si30 groups and the high-dose groups of the Si600 compared with the control group. But no significant changes in the RBC number and HGB level were found in the four sizes of silica particles.

Inflammatory Reaction for Rats After Intratracheal Instillation of Silica Particles

As shown in Fig. 3, after particles instillation, there was a significant increase in hs-CRP, TNF-α, IL-1β, and IL-6 levels in all expression groups of four sizes of silica particles compared with the control group. At the same-size particle groups, increasing the dose of silica particles could cause significant elevation of the hs-CRP levels (Fig. 3a). The hs-CRP levels in serum in the middle- and high-dose groups of four sizes of particles were significantly up-regulated when compared with the low-dose groups; the hs-CRP levels in serum in the high-dose groups of four sizes of particles were higher than those of in the middle-dose groups of four sizes of particles. And a significant increase in the levels of TNF-α and IL-1β measured in serum was found in high-dose groups of Nano-Si90, Nano-Si60, and Nano-Si30 compared with low-dose groups. There was a significant increase in IL-6 levels in the high-dose groups of Nano-Si30 and Si600 compared with the low- and middle-dose groups.

But at the same-dose groups, the hs-CRP levels in serum in the middle- and high-dose groups of Nano-Si90, Nano-Si60, and Nano-Si30 were significantly up-regulated when compared with those of the Si600. A significant increase in hs-CRP levels were found in the middle- and high-dose groups of Nano-Si30 compared with Nano-Si90 and Nano-Si60. The IL-1β levels in high-dose groups of Nano-Si60 and Nano-Si30 were significantly up-regulated compared with Si 600. The IL-6 levels in all experimental groups of Nano-Si30, the high- and low-dose groups of Nano-Si60 and the middle-dose groups of Nano-Si90 were significantly up-regulated when compared with Si 600. All these results manifested that the levels of hs-CRP in serum increased in both dose-dependent and size-dependent manner.

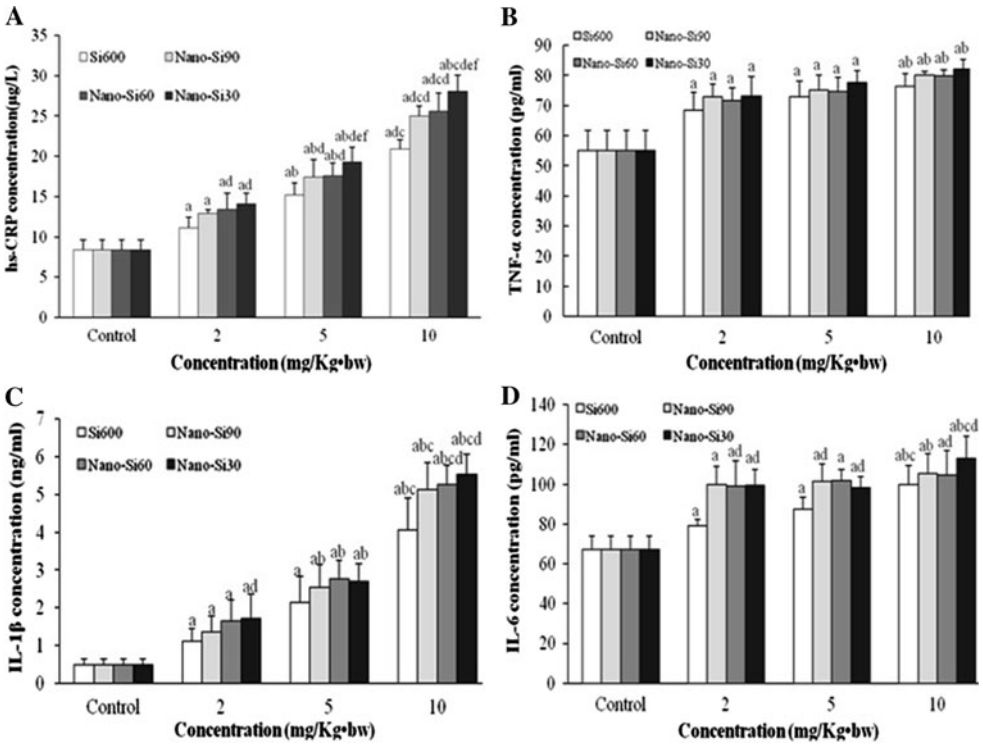

Fig. 3 The hs-CRP levels and cytokine profile in serum after intratracheal instillation of silica particles. As shown, after particles instillation, there was a significant increase in hs-CRP (**a**), TNF-α (**b**), IL-1β (**c**) and IL-6 (**d**) levels in all expression groups of four sizes of silica particles. [a]$p < 0.05$, versus control group; [b]$p < 0.05$, versus the same-size group (2 mg/Kg bw); [c]$p < 0.05$, versus the same-size group (5 mg/Kg bw); [d]$p < 0.05$, versus the same-dose group (600 nm); [e]$p < 0.05$, versus the same-dose group (90 nm) and [f]$p < 0.05$, versus the same-dose group (60 nm)

Oxidative Stress for Rats After Intratracheal Instillation of Silica Particles

As shown in Fig. 4a, compared with the control group, the ROS levels of the four sizes of particles elevated significantly. At the same-size particle groups, increasing the dose of silica particles could cause significant elevation of the ROS levels. The ROS levels in serum in the middle- and high-dose groups of four sizes of particles were significantly up-regulated when compared with the low-dose groups, the ROS levels in serum in the high-dose groups of four sizes of particles were higher than those of in the middle-dose groups of four sizes of particles. But at the same-dose groups, the ROS levels in serum in the middle- and high-dose groups of Nano-Si90, Nano-Si60, and Nano-Si30 were significantly up-regulated when compared with those of the Si600 groups. All these results manifested that the levels of ROS in serum increased in both dose-dependent and size-dependent manner.

There was a significant increase in the MDA levels in the middle- and high-dose groups of Nano-Si90, Nano-Si60, and Nano-Si30, and the high-dose groups of Si 600 compared with the control group (Fig. 4b). The MDA levels in the high-dose groups of Nano-Si60 and Nano-Si30 were higher than that in the middle- and low-dose groups. In the high-dose groups of Nano-Si90 and Si 600, there was a significant increase in the MDA levels compared with the low-dose group. Compared with the control group, the SOD levels of the middle- and high-dose groups of Nano-Si60, Nano-Si30 and the high-dose groups of Nano-Si90 decreased significantly. There was a significant decrease in the GSH-Px levels in the high-dose groups of four-size particle groups compared with the control group. But there was no significant change in all experimental groups of four-size particle groups.

Effects of Four Sizes of Particles After Exposure on Endothelial Dysfunction and Blood Coagulation in Blood in Rats

As shown in Fig. 5, after particles instillation, there was a significant increase in the levels of D-dimer, ET-1, and P-selectin in all experimental groups of four sizes of silica particles compared with the control group. At the same-size particle groups, the levels of D-dimer and ET-1 in the high-dose groups of four sizes of silica particles were higher than those in the middle- and low-dose groups. The levels of P-selectin in the high-dose groups of Nano-Si90, Nano-Si60, and Nano-Si30 were higher than those in the middle- and low-dose groups (Fig. 5c). There was a significant increase in the levels of P-selectin in the high-dose groups of Si600 compared with the low-dose groups. Furthermore, the levels of D-dimer, ET-1, and P-selectin of the middle-dose groups of Nano-Si90, Nano-Si60, and Nano-Si30 significantly elevated when compared with the low-dose groups. At the same-dose groups, the levels of D-dimer and ET-1 in the high-dose groups of Nano-Si30, the middle- and high-dose groups of Nano-Si90 and Nano-Si60 and the

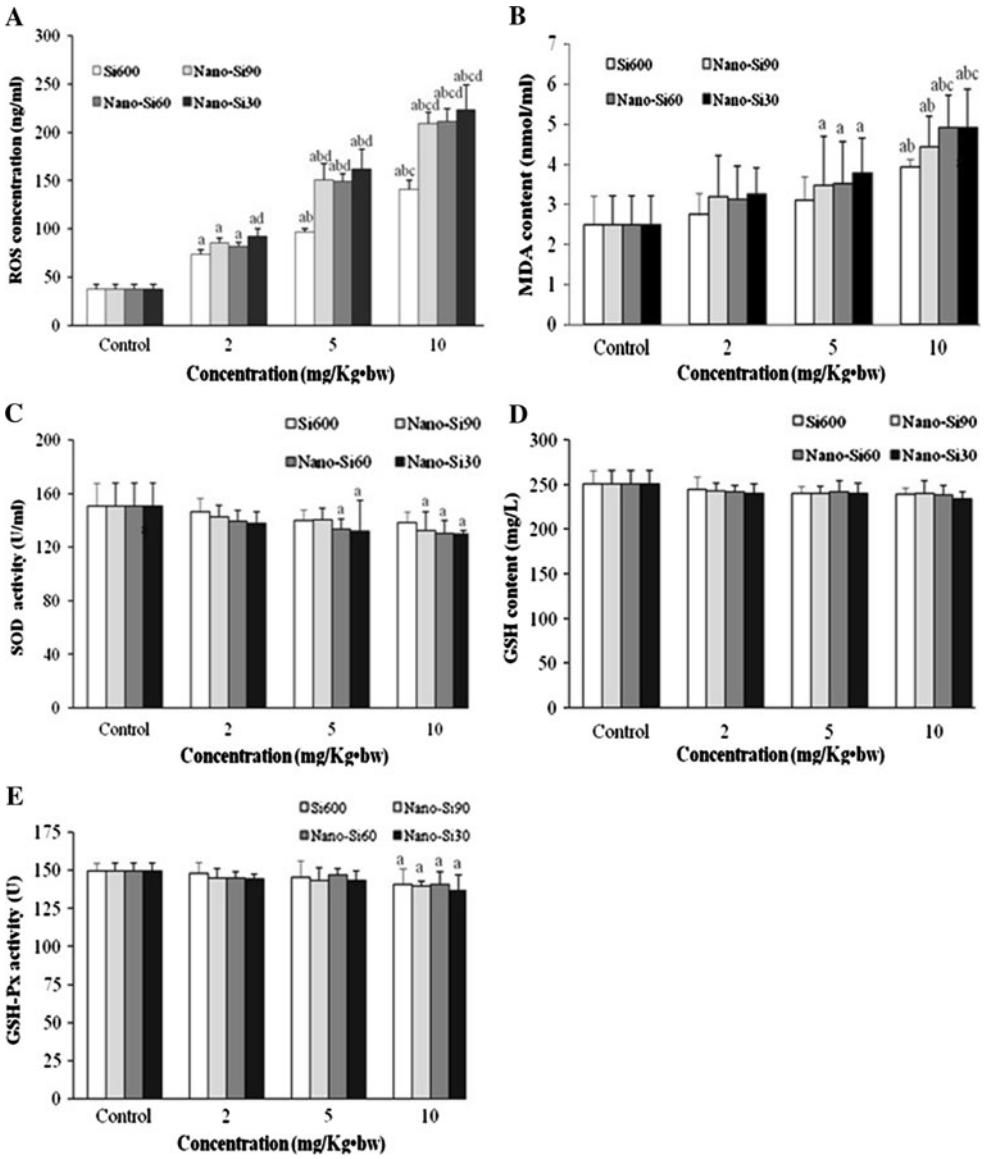

Fig. 4 Oxidative stress biomarkers responses of four sizes of silica particles of serum in rats after exposure. Effects of 600, 90, 60, and 30 nm of silica particles with concentrations from 2 to 10 mg/Kg bw on ROS levels (**a**), MDA levels (**b**), SOD levels (**c**), GSH levels (**d**) and GSH-Px levels (E). $^{a}p < 0.05$, versus control group; $^{b}p < 0.05$, versus the same-size group (2 mg/Kg bw); $^{c}p < 0.05$, versus the same-size group (5 mg/Kg bw); $^{d}p < 0.05$, versus the same-dose group (600 nm)

levels of P-selectin in the high-dose groups of Nano-Si30 significantly increased when compared with the Si60. Besides, compared with the high-dose groups of Nano-Si90 and Nano-Si60, there was a significant increase in the levels of ET-1 and P-selectin in the high-dose groups of Nano-Si30.

As shown in Fig. 6, except in low-dose groups of Si600, there was a significant increase in the levels of sICAM-1 and sVCAM-1 in all expression groups of four sizes of silica particles compared with the control groups. At the same-size particle groups, the levels of sICAM-1 in the high-dose group of four sizes of silica particles significantly increased. There was a significant increase in the levels of sICAM-1 in the middle-dose groups of Nano-Si90, Nano-Si60, and Nano-Si30 compared with the low-dose groups. Further, the levels of sICAM-1 in the middle- and high-dose groups of Nano-Si90, Nano-Si60, and Nano-Si30 significantly elevated when compared with Si600. Compared with the middle-dose groups, there was a significant increase in the levels of sVCAM-1 in the high-dose groups of Nano-Si60 and Nano-Si30. However, only the levels of sVCAM-1 in the high-dose groups of Nano-Si90, Nano-Si60, and Nano-Si30 were significantly elevated when compared with the Si600 . Thus, all these results manifested that the levels of sICAM-1 and sVCAM-1 in serum increased in both dose- and size-dependent manner.

As shown in Fig. 7, after four sizes of silica particles instillation, there was a significant decrease in the levels of NO and the activity of NOS and eNOS in all experimental groups of four sizes of silica particles compared with the control groups. But except the low dose of four sizes of particles and the middle dose of Si600, the activity of iNOS in the other groups was significantly up-regulated when

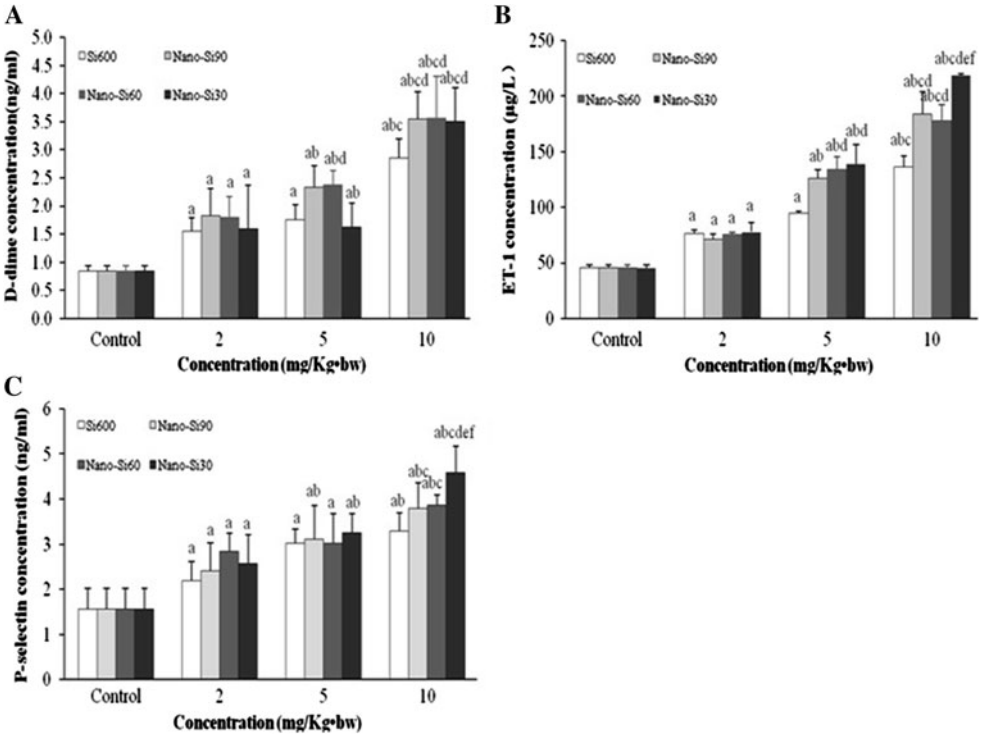

Fig. 5 The result of D-dimer (**a**), ET-1 (**b**) and P-selectin (**c**) levels after exposure to 600, 90, 60 and 30 nm of silica particles with concentrations from 2 to 10 mg/Kg bw. [a] $p < 0.05$, versus control group; [b] $p < 0.05$, versus the same-size group (2 mg/Kg bw); [c] $p < 0.05$, versus the same-size group (5 mg/Kg bw); [d] $p < 0.05$, versus the same-dose group (600 nm); [e] $p < 0.05$, versus the same-dose group (90 nm) and [f] $p < 0.05$, versus the same-dose group (60 nm)

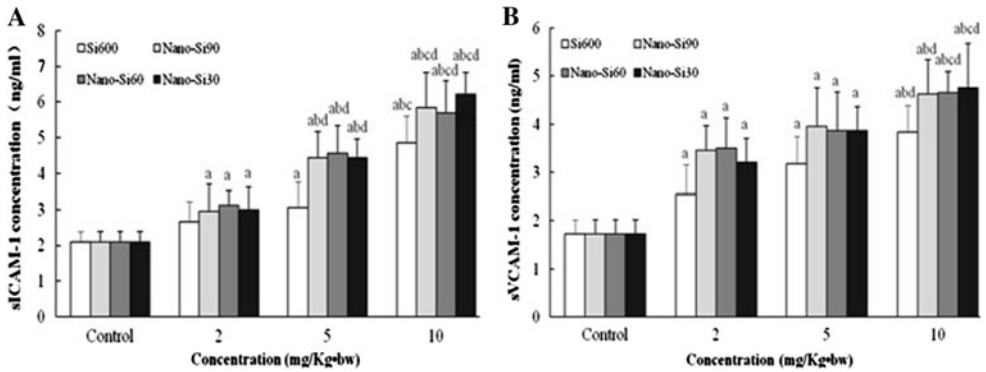

Fig. 6 The levels of sICAM-1 and sVCAM-1 in serum after intratracheal instillation of silica particles. **a** sICAM-1 levels were measured after the cells exposure to 600, 90, 60, and 30 nm of silica particles with concentrations from 2 to 10 mg/Kg bw. **b** sVCAM-1 levels were measured after the cells exposure to 600, 90, 60, and 30 nm of silica particles with concentrations from 2 to 10 mg/Kg bw. [a] $p < 0.05$, versus control group; [b] $p < 0.05$, versus the same-size group (2 mg/Kg bw); [c] $p < 0.05$, versus the same-size group (5 mg/Kg bw); [d] $p < 0.05$, versus the same-dose group (600 nm)

compared with the control groups. In the same-size particle groups, the levels of NO in the high-dose groups of four sizes of silica particles and middle-dose groups of Nano-Si90, Nano-Si60, and Nano-Si30 were significantly down-regulated, when compared with the low-dose groups. In the same-dose groups, the levels of NO in the high- and middle-dose groups of Nano-Si90, Nano-Si60, and Nano-Si30 were lower than that in the Si600 , and there was a significant decrease in the levels of NO in the high-dose group of Nano-Si30 compared with Nano-Si90 and Nano-Si60. In the same-size groups, there was a significant decrease in the activity of NOS and eNOS in the high-dose groups of Nano-Si90, Nano-Si60, and Nano-Si30. In the same-dose groups, compared with Si600, only the activity of NOS and eNOS in the high-dose groups of Nano-Si60 and Nano-Si30 and the activity of NOS in the high-dose groups of Nano-Si90 were significantly down-regulated. However, in the same-size groups, there was a significant increase in the activity of iNOS in the high-dose groups of Nano-Si90, Nano-Si60, and Nano-Si30 compared with the low- and middle-dose groups. In the high-dose groups, the activity of iNOS of Nano-Si90, Nano-Si60, and Nano-Si30 was higher

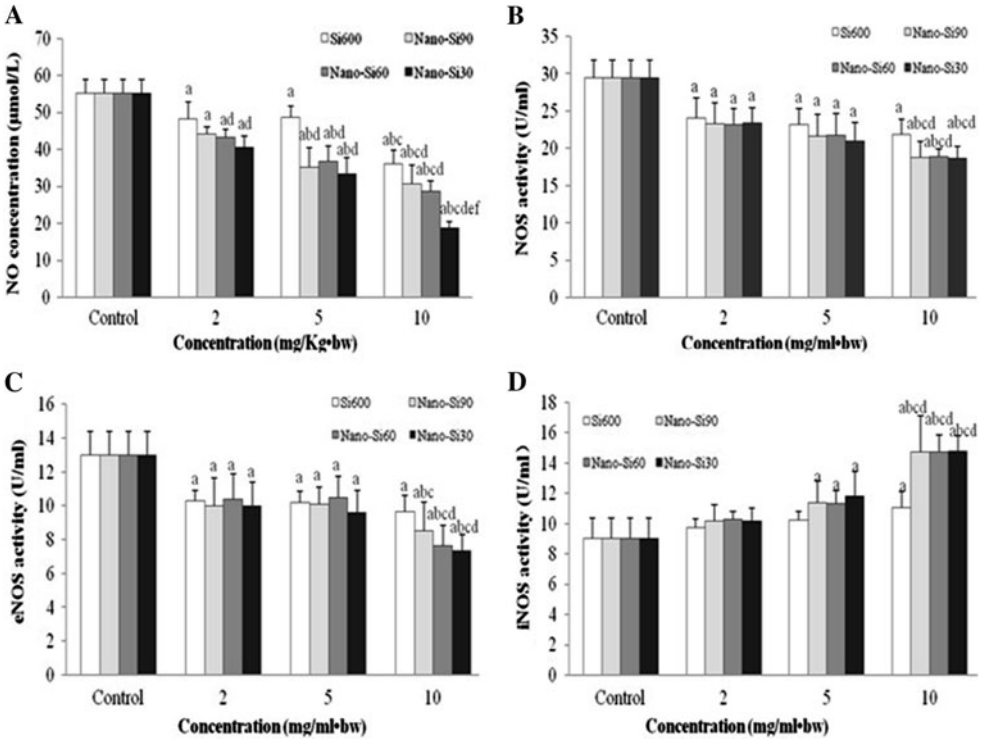

Fig. 7 Effects of four sizes of silica particles on the levels of NO (**a**) and the activity of NOS (**b**), eNOS (**c**) and iNOS (**d**) in blood serum in rats after exposure. [a]$p < 0.05$, versus control group; [b]$p < 0.05$, versus the same-size group (2 mg/Kg bw); [c]$p < 0.05$, versus the same-size group (5 mg/Kg bw); [d]$p < 0.05$, versus the same-dose group (600 nm); [e]$p < 0.05$, versus the same-dose group (90 nm) and [f]$p < 0.05$, versus the same-dose group (60 nm)

than the Si600 . All these results manifested that the concentration of Si in serum and hearts increased in both dose- and size-dependent manner.

Effects of Four Sizes of Particles After Exposure on the Myocardial Enzymes in Serum in Rats

As shown in Fig. 8, there was a significant increase in the activity of CK-MB and LDH in all experimental groups compared with the control groups after four sizes of silica particles instillation. In the same-size groups, there was a significant increase in the activity of CK-MB and LDH in the high-dose groups of four-size particle groups. The activity of LDH in the middle-dose groups of four-size particle groups was higher than that in the low-dose groups. In the same-dose groups, only in the high-dose groups of Nano-Si30, the activities of CK-MB and LDH were significantly up-regulated when compared with the Si600.

Discussion

Size, surface, area, and number of particles appear to play important roles in facilitating nanosized particle-related toxicity [2, 19]. The size of the particles plays a key role in their adhesion to and interaction with biological cells [20]. Si600, Nano-Si90, and Nano-Si60 exhibited very good monodispersity in the experiment, while Nano-Si130 agglomerated slightly due to their high surface activity.

All the four particles were found in the blood circulation and hearts (Table 3). Moreover, our results showed that the Si content effect in the blood circulation and heart produced by silica particles were strongly related to particle size and dosage. Compared to conventional size particles, silica nanoparticles more easily enter the cardiovascular system. The ultrafine particles can translocate from the lung to the systemic circulation by crossing the alveolar-capillary barrier [21], and the inhaled nanoparticles could be translocated into the blood circulation, thus, providing a possible mechanism for the cardiovascular toxicity of particles matter [22].

Many studies had demonstrated that particulate air pollutants were shown to trigger pro-inflammatory signaling via an ROS-dependent mechanism in lungs [14, 23, 24]. Considering the possibility that nanoparticles are capable of reaching the heart and other remote organs via the vasculature [22], particle-mediated toxic effects could be realized at the level of the cardiovascular. Different kinds of nanomaterials, such as fullerenes, single-wall carbon nanotubes (SWCNTs), quantum dots (QDs), etc., can induce ROS production in in vivo or in vitro experiments [21]. And current research suggests that the generation of ROS caused by particles is one of the possible mechanisms leading to cardiovascular dysfunction [5, 11]. The present study showed that the levels of both ROS and

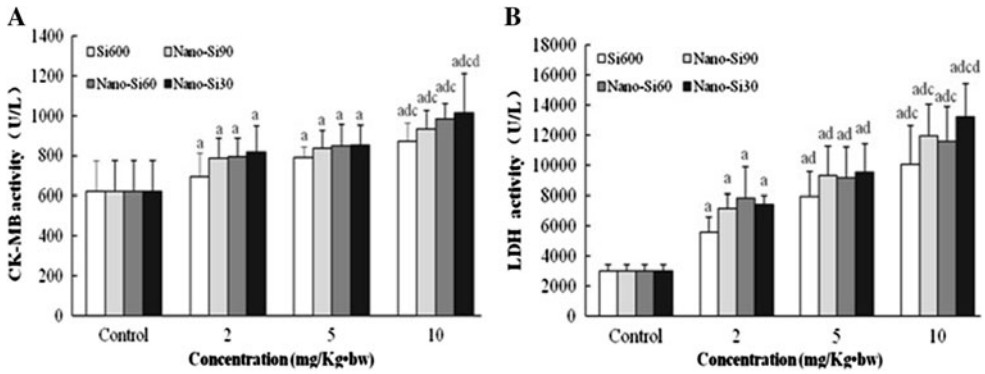

Fig. 8 Effects of four sizes of silica particles on the activities of CK-MB and LDH in serum in rats after exposure. **a** CK-MB levels were measured after the cells exposure to 600, 90, 60, and 30 nm of silica particles with concentrations from 2 to 10 mg/Kg bw. **b** LDH levels were measured after the cells exposure to 600, 90, 60, and 30 nm of silica particles with concentrations from 2 to 10 mg/Kg bw. $^{a}p < 0.05$, versus control group; $^{b}p < 0.05$, versus the same-size group (2 mg/Kg bw); $^{c}p < 0.05$, versus the same-size group (5 mg/Kg bw); $^{d}p < 0.05$, versus the same-dose group (600 nm)

MDA in serum induced by the four silica particles increased in a dose-dependent manner (Fig. 4a, b), and the activities of SOD and GSH-Px decreased (Fig. 4c, e). The results suggested that oxidative stress could be one of the most important toxicity mechanisms related to nanoparticles exposure. These results were similar to numerous previous studies [25]. But there are several studies that oppose this phenomenon [26]. Increased amounts of ROS were shown to be closely involved in myocardial stunning, necrosis, vascular dysfunction, apoptosis, and some of their effects were effectively blocked by free radical scavengers.

Moreover, compared with micro-scaled silica particles, silica nanoparticles were more prominent role at high-dose levels. A large number of studies have shown that the specific surface area of nanoparticles has a direct relationship with the ability of inducing ROS and inflammatory response [14]. These special physicochemical properties of silica nanoparticles enhanced its chemical activity and biological activity and caused more serious cardiovascular injury compared with micro-scaled silica particles.

The present study showed that the levels of WBC and PLT significantly increased in blood in a size- and dose-dependent manner, while the levels of RBC and HGB had no significant changes (Fig. 2), which hinted the systemic inflammation. Stimulation of the liver that responds with the production and the release of acute phase proteins such as CRP is an early and integral part of the systemic inflammatory response. These proteins are stimulated by circulating cytokines and/or ROS, particularly IL-1β, IL-6, and TNF-α [27, 28]. Many studies have suggested that C-reactive protein (CRP) is an important and independent predictor of cardiovascular disease [29]. It has been shown that increased levels of CRP resulting from exposure to particles matter are involved in the infiltration of monocytes into the arterial wall, which promotes atherogenesis by amplifying inflammatory and procoagulant responses [30]. The present results showed the levels of hs-CRP increased in a size-dependent manner following the four silica particles exposure (Fig. 3a), which indicated that silica nanoparticles could cause inflammations in the cardiovascular system compared with conventional scale silica particles, and the smaller the particle size, the more obvious responses.

Cytokines play an important role in regulating immunity and are classified into proinflammatory (TNF-α, IL-6, and IL-1β) [31]. The present results showed that the inflammatory cytokines (Fig. 3b, c, d), which hint that the inflammatory reaction appears after rats exposed to silica particles. Several studies have shown that exposures to nanoscaled particles produce greater inflammatory when compared to exposure to larger-sized particles at equivalent mass concentration [2, 32]. Amorphous silica nanoparticles increase transient inflammatory response after intratracheal instillation [33, 34] and induced pro-inflammatory response like IL-6, IL-1β, and TNF-α release.

Reactive nitrogen species may also be involved in endothelial inflammation induced by nanoparticles. Interestingly, a recent study has demonstrated that exogenous Zn elicits an endothelial stress response, which resembles that of nitric oxide-mediated nitrosative stress [35]. The dysfunction of endothelial cells may be explained by the likely induction of ROS and reactive nitrogen species induced by nanoparticles. The present study showed that the increase in ROS level (Fig. 4a), the decrease in endogenous NO production, and activities of NOS and eNOS in serum were found by silica nanoparticles exposure (Fig. 7), which further indicate that nanoparticles can induce oxidative stress (Fig. 4). It is known that superfluous ROS may react with NO in the process of producing highly reactive and cytotoxic nitrogen products, such as

peroxynitrite (ONOO–) and peroxynitrous acid (ONOOH). Peroxynitrite can in turn react with lipids, DNA, and proteins, resulting in severe oxidative injuries. Thus, once the nanoparticles enter the blood circulation, the generated free radicals would oxidize low-density lipoprotein (LDL)/lipid to generate peroxidized lipoproteins. NO induces vasodilatation in the cardiovascular, prevents neutrophil/platelet adhesion to endothelial cells, inhibits platelet aggregation, controls smooth muscle cell proliferation and migration, maintains an endothelial cell barrier function, and regulates programmed cell death (apoptosis) [36]. In general, iNOS was expressed in normal tissues less, but iNOS was expressed in multiple tissues induced by inflammation, tumor, degeneration, and many other disease states. Therefore, the level of iNOS in serum may reflect the internal environment of the body stability, and high expression reflected that the body may be in a state of stress. Serum eNOS was mainly produced by vascular endothelial cells, so in serum the level of eNOS could be roughly reflected endothelial cell function state. The present results showed that silica particles exposure decreased the production and release of NO from serum in rats, accompanied with down-regulating NOS and eNOS activity and up-regulating iNOS activity (Fig. 7). Although the level of NO in the serum could not accurately reflect the ability of endothelial cells to release NO, the level of decrease can be used to the prediction index to judge the system or organization of NOS/NO system disorder. In this study, the serum levels of NO in high-dose group were decreased in a size and dose-dependent manner. Compared with the control group, the serum levels of iNOS were elevated in all the experimental groups, and the levels of iNOS in high dose of silica nanoparticles groups were significantly higher than in Si600, which prompted silica particles exposure may cause or worsen organism or tissue stress. Furthermore, the increase of iNOS activity produces a large number of NO, which exacerbate the endothelial NO/NOS system status, and the change induced by nano-scaled silica particles was more serious.

Endothelial cell injury can cause ICAM-l and VCAM-l expression increases, which can reflect the tendency to thrombosis. Stimulated adhesion molecules can secret some soluble chemical agent, such as monocytes, inflammatory protein, and IL-8, which could affect endothelial cells; meanwhile, the activity of the endothelial cells can affect the generation of the various types of adhesion factors and chemical inducers. Moreover, the oxidized lipoprotein in plasma may induce the intensive expression of adhesion molecules (e.g., VCAM-1, ICAM-1) and aggravate monocyte adhesion [37]. In the present study, the levels of sICAM-1 and sVCAM-l expression in all groups elevated in a dose-dependent manner (Fig. 6). In addition, all experimental group P-selectin expression level significantly elevated, and three experimental nanoscaled groups increased in a dose-dependent manner (Fig. 5). P-selectin was a mark of coagulation system disorders. This present study showed that adhesion molecule expression significantly elevated after exposure to silica particles, and the increase in adhesion molecules and some related cytokines expression promoted inflammatory cells on endothelial adhesion contributing to endothelial injury. The study also showed that the effect of silica nanoparticles on rat endothelial function in rats was significantly higher than micro-scaled silica particles.

ET-1 was significantly related to atherosclerosis, and studies have found that plasma ET-1 in heart failure patients increased manifold [38, 39]. This present experiment showed that the ET-l levels in plasma of rats markedly elevated with the increases of exposure dose. The levels of ET-1 in plasma in all experimental groups increased in both dose- and size-dependent manner (Fig. 5). We also found that the D-dimer levels in plasma of Wistar rats increased significantly after intratracheal instillation of four kinds of silica particles, and in middle- and high-dose groups, the levels of D-dimer in silica nanoparticles groups were significantly higher than that of Si600 (Fig. 5). D-dimer is a fibrin degradation product, a small protein fragment present in the blood after a blood clot is degraded by fibrinolysis. The levels of increase in D-dimer in plasmin indicated that there are thrombosis in vivo and the existence of secondary fibrinolysis. D-dimer levels directly related to the cardiac events after myocardial infarction, and the PLT level increased in blood in a size- and dose-dependent manner (Fig. 2). The present results suggest that nanometer silica particle exposure could alter coagulation/fibrinolytic system stability, and the effect from nanometer silica particle was significantly higher than that of micron silica particles.

In the normal state, myocardial cell contained a large number of enzymes, such as creatine kinase (CK), lactate dehydrogenase (LDH), when myocardial cell damaged or necrosis, intracellular enzymes would be released into the blood circulation and elevated the serum levels of myocardial enzyme [40]. The present results showed that the levels of myocardial enzyme LDH and CK-MB in serum of all experimental groups significantly increased compared with control group, and in high-dose groups, they were higher than those of low- and middle-dose groups, which suggested that myocardial in rat may have damage and ischemic necrosis. In the high-dose group, the levels of myocardial enzyme LDH and CK-MB in Nano-Si30 groups were significantly higher than those in Si600, which mean high dose of Nano-Si30 is more prone to induce myocardial damage.

Based on the present experiment, we summarized the dosage of silica particles for each effect endpoint

Table 4 The dosage of silica particles for each effect endpoint

Effect endpoints	Si600 nm (mg/Kg bw)	Nano-Si90 (mg/Kg bw)	Nano-Si60 (mg/Kg bw)	Nano-Si30 (mg/Kg bw)
Hematology parameters				
White blood cells (WBC)	2	2	2	2
Red blood cells (RBC)	10	2	2	2
Hemoglobin (HGB)	10	2	5	2
Platelets (PLT)	2	2	2	2
Oxidative stress				
Reactive oxygen species (ROS)	2	2	2	2
Malondialdehyde (MDA)	10	5	5	5
Superoxide dismutase (SOD)	10	10	5	5
Glutathione peroxidase (GSH-Px)	10	10	10	10
Inflammatory reaction				
High-sensitivity C-reactive protein (hs-CRP)	2	2	2	2
Tumor necrosis factor-alpha (TNF-α)	2	2	2	2
Interleukin-1beta (IL-1β)	2	2	2	2
Interleukin-6 (IL-6)	2	2	2	2
Blood coagulation				
D-dimer	2	2	2	2
Endothelin-1 (ET-1)	2	2	2	2
P-selectin	2	2	2	2
Endothelial dysfunction				
Intercellular adhesion molecule-l (ICAM-l)	5	2	2	2
Vascular cell adhesion molecule-l (VCAM-l)	2	2	2	2
NO/NOS system	2	2	2	2
Myocardial enzyme				
Lactate dehydrogenase (LDH)	2	2	2	2
MB isoenzyme of creatine kinase (CK-MB)	2	2	2	2

(Table 4). We found an interesting event that four sizes of silica particles in low dosage (2 mg/Kg bw) could induce the toxic effects of cardiovascular system; however, the toxic effect has no significant difference among the low dosage of the particles. We speculate that prolonged inhalation of silica particles with low dose ($\leq$2 mg/Kg bw) could cause cardiovascular toxicity effects, with the increase in the concentration of particles, the smaller the particles size, toxic effects are more obvious.

Conclusion

Intratracheal instillation of silica nanoparticles can pass through the alveolar-capillary barrier into systemic circulation. There were dose- and size-dependent cardiovascular toxicity in male Wistar Rats after exposure to different sizes of silica nanoparticles. Heart is a target organ of silica nanoparticles. Intratracheal instillation of silica nanoparticles can cause inflammatory reaction, oxidative stress, and endothelial dysfunction. ROS generation in the cardiovascular could be one of the mechanisms responsible for the cardiovascular toxic effects of silica nanoparticles. In addition, we firstly found endothelial NO/NOS system disorder caused by nanoparticles could be one of the mechanisms for endothelial dysfunction. The results will provide a scientific basis to evaluate the risk of silica particles in the ecosystem and to human health.

Acknowledgments The authors would like to thank Prof. Wensheng Yang, and Dr. Jianquan Xu from Jilin University for the preparation of silica particles. This work was supported by Grant of Specialized Research Fund for the Doctoral Program of Higher Education (20090061110062) and Jilin University Research Foundation for Basic Science (200903112).

Conflict of interest The authors declare that there are no conflicts of interest. The authors alone are responsible for the content and writing of the paper.

References

1. Nel, A., Xia, T., Madler, L., & Li, Ning. (2006). Toxic potential of materials at the nanolevel. *Science, 311*, 622–627.
2. Oberdörster, G., Oberdorster, E., & Oberdörster, J. (2005). Nanotoxicology: An emerging discipline evolving from studies of ultrafine particles. *Environmental Health Perspectives, 113*(7), 823–839.
3. Li, Y., Sun, L., Sun, Z. W., Jin, M. H., & Du, Z. J. (2011). Size-dependent cytotoxicity of amorphous silica nanoparticles in human hepatoma HepG2 cells. *Toxicology in Vitro, 25*(7), 1343–1352.
4. LeBlanc, A. J., Cumpston, J. L., Chen, B. T., Frazer, D., Castranova, V., & Nurkiewicz, T. R. (2010). Nanoparticle inhalation impairs endothelium-dependent vasodilation in subepicar-

dial arterioles. *Journal of Toxicology and Environmental Health Part A, 72*(24), 1576–1584.
5. Zhu, M. T., Wang, B., Yuan, L., et al. (2011). Endothelial dysfunction and inflammation induced by iron oxide nanoparticle exposure: Risk factors for early atherosclerosis. *Toxicology Letters, 203*, 162–171.
6. Kleinman, M. T., Araujo, J. A., Nel, A., Sioutas, C., Campbell, A., Cong, P. Q., et al. (2008). Inhaled ultrafine particulate matter affects CNS inflammatory processes and may act via MAP kinase signaling pathways. *Toxicology Letters, 178*, 127–130.
7. Nurkiewicz, T. R., Porter, D. W., Hubbs, A. F., & Chen, B. T. (2008). Nanoparticle inhalation augments particle-dependent systemic microvascular dysfunction. *Part Fibre Toxicology, 5*, 1.
8. Samet, J. M., Dominici, F. R., & Curriero, F. C. D. (2000). Fine particulate air pollution and mortality in 20 US cities, 1987–1994. *New England Journal of Medicine, 343*, 1742–1749.
9. Stern, S. T., & McNeil, S. E. (2008). Nanotechnology safety concerns revisited. *Toxicological Sciences, 101*, 4–21.
10. Gauderman, W. J., Avol, E., & Gilliland, F. (2004). The effect of air pollution on lung development from 10 to 18 years of age. *New England Journal of Medicine, 351*, 1057–1067.
11. Ni, Bai., Majid, Khazaei., van Eeden, S. F., & Laher, I. (2007). The pharmacology of particulate matter air pollution-induced cardiovascular dysfunction. *Pharmacology & Therapeutics, 113*, 16–29.
12. Navarro, E., Piccapietra, F., Wagner, B., Marconi, F., Kaegi, R., Odzak, N., et al. (2008). Toxicity of silver nanoparticles to Chlamydomonas reinhardtii. *Environmental Science and Technology, 42*(23), 8959–8964.
13. Hamilton, J. M., Salmon, D. P., Galasko, D. R. R., Emond, J., Hansen, L. A., Masliah, E., et al. (2008). Visuospatial deficits predict rate of cognitive decline in autopsy-verified dementia with Lewy bodies. *Neuropsychology, 22*(6), 729–737.
14. Dick, C. A., Singh, P., Daniels, M., Evansky, P., Becker, S., & Gilmour, M. I. (2003). Murine pulmonary inflammatory responses following instillation of size-fractionated ambient particulate matter. *Journal of Toxicology and Environmental Health Part A, 66*(23), 2193–2207.
15. Bai, J., Chiu, W., Wang, J., Tzeng, T., Perrimon, N., & Hsu, J. (2001). The cell adhesion molecule Echinoid defines a new pathway that antagonizes the Drosophila EGF receptor signaling pathway. *Development, 128*(4), 591–601.
16. Sun, Q., Wang, A., Jin, X., Natanzon, A., Duquaine, D., & Brook, R. D. (2005). Long-term air pollution exposure and acceleration of atherosclerosis and vascular inflammation in an animal model. *The Journal of American Medical Association, 294*, 3003–3010.
17. Arts, J. H., Muijser, H., Duistermaat, E., Junker, K., & Kuper, C. F. (2007). Five-day inhalation toxicity study of three types of synthetic amorphous silicas in Wistar rats and post-exposure evaluations for up to 3 months. *Food and Chemical Toxicology, 45*, 1856–1867.
18. Park, E. J., & Park, K. (2009). Oxidative stress and pro-inflammatorty responses induced by silica nanoparticles in vivo and in vitro. *Toxicology Letters, 184*, 18–25.
19. Liu, Y., Jiao, F., Qiu, Y., Dong, J. Q., Zhao, Yl., Chen, C. Y., et al. (2009). The effect of Gd @ $C_{82}(OH)_{22}$ nanoparticles on the release of Th1/Th2 cytokines and induction of TNF-α mediated cellular immunity. *Biomaterials, 30*, 3934–3945.
20. Braydich-Stolle, L., Hussain, S., Schlager, J. J., & Hofmann, M. (2005). In vitro cytotoxicity of nanoparticles in mammalian germline stem cells. *Toxicological Sciences, 88*, 412–419.
21. Foster, K. A., Yazdanian, M., & Audus, K. L. (2001). Microparticulate uptake mechanisms of in vitro cell culture models of the respiratory epithelium. *Journal of Pharmacy and Pharmacology, 53*, 57–66.
22. Oberdörster, G., Sharp, Z., Atudorei, V., Elder, A., Gelein, R., Lunts, A., et al. (2002). Extrapulmonary translocation of ultrafine carbon particles following wholebody inhalation exposure of rats. *Journal of Toxicology and Environmental Health Part A, 65*, 1531–1543.
23. Seaton, A., MacNee, W., & Donaldson, K. (1995). Particulate air pollution and acute health effect. *Lancet, 345*(8943), 176–178.
24. Donaldson, K., & Stone, V. (2003). Current hypotheses on the mechanisms of toxicity of ultrafine particles. *Annali dell Istituto Superiore di Sanita, 39*, 405–410.
25. Schins, P. F., Lightbody, J. H., Borm, P. J. A., Shi, T., Donaldson, K., & Stone, V. (2004). Inflammatory effects of coarse and fine particulate matter in relation to chemical and biological constituents. *Toxicology and Applied Pharmacology, 195*, 1–11.
26. Lin, W., Huang, Y. W., Zhou, X. D., & Ma, Y. (2006). In vitro toxicity of silica nanoparticles in human lung cancer cells. *Toxicology and Applied Pharmacology, 217*, 252–259.
27. Yuan, X. M., & Li, W. (2008). Iron involvement in multiple signaling pathways of atherosclerosis: A revisited hypothesis. *Current Medicinal Chemistry, 15*(21), 2157–2172.
28. Ramage, L., Proudfoot, L., & Guy, K. (2004). Expression of C-reactive protein in human lung epithelial cells and upregulation by cytokines and carbon particles. *Inhalation Toxicology, 16*, 607–613.
29. Ramage, L., & Guy, K. (2004). Expression of C-reactive protein and heat-shock protein-70 in the lung epithelial cell line A549, in response to PM10 exposure. *Inhalation Toxicology, 16*, 447–452.
30. Fibrinogen Studies Collaboration. (2007). Associations of plasma fibrinogen levels with established cardiovascular disease risk factors, inflammatory markers, and other characteristics: Individual participant meta-analysis of 151, 211 adults in 31 prospective studies. *American Journal of Epidemiology, 166*, 867–879.
31. Libby, P. (2002). Inflammation in atherosclerosis. *Nature, 420*, 868–874.
32. Lindmark, E., Diderholm, E., & Wallentin, L. (2001). Relationship between interleukin 6 and mortality in patients with unstable coronary artery disease: Effects of an early invasive or noninvasive strategy. *The Journal of American Medical Association, 286*, 2107–2113.
33. Wang, J., Zhou, G., Chen, C., & Yu, H. (2007). Acute toxicity and biodistribution of different sized titanium aioxide particles in mice after oral administration. *Toxicology Letters, 168*, 176–185.
34. Cao, Q., Zhang, S., Dong, C., & Song, W. (2007). Pulmonary responses to fine particles: Different between the spontaneously hypertensive rates and wistar Kyoto rats. *Toxicology Letters, 171*, 126–137.
35. Cho, W. S., Choi, M., Han, B. S., & Jeong, J. (2007). Inflammmatory mediators induced by intratracheal instillation of ultrafine amorphous silica particles. *Toxicology Letters, 175*, 24–33.
36. Wiseman, D. A., Wells, S. M., Wilham, J., Hubbard, M., Welker, J. E., & Black, S. M. (2006). Endothelial response to stress from exogenous Zn^{2+} resembles that of NO-mediated nitrosative stress, and is protected by MT-1 overexpression. *American Journal of Physiology and Cell Physiology, 291*, C555–C568.
37. Chung, H. T., Pae, H. O., Choi, B. M., Billiar, T. R., & Kim, Y. M. (2001). Nitric oxide as a bioregulator of apoptosis. *Biochemical and Biophysical Research Communications, 282*, 1075–1079.
38. Hsiai, T. K., Cho, S. K., Reddy, S., Hama, S., Navab, M., Demer, L. L., et al. (2001). Pulsatile flow regulates monocyte adhesion to oxidized lipid-induced endothelial cells. *Arteriosclerosis, Thrombosis, and Vascular Biology, 21*, 1770–1776.
39. Zhang, X. Y., Yin, J. L., & Cheng, K. (2010). Biodistribution and toxicity of nanodiamonds in mice after intratracheal instillation. *Toxicology Letters, 198*, 237–243.
40. Karacalioglu, O., Arslan, Z., & Kilie, S. (2007). Baseline serum levels of cardiac biomarkers in patients with stable coronary artery disease. *Biomarkers, 12*(5), 533–540.